A&A 422, 323–330 (2004)
DOI: 10.1051/0004-6361:20035712

Astronomy & Astrophysics

Electron acceleration and radiation in evolving complex active regions

A. Anastasiadis[1], C. Gontikakis[2], N. Vilmer[3], and L. Vlahos[4]

[1] National Observatory of Athens, Institute for Space Applications and Remote Sensing, 152 36 Penteli, Greece
[2] Research Center for Astronomy and Applied Mathematics, Academy of Athens, Greece
e-mail: cgontik@cc.uoa.gr
[3] LESIA, Observatoire de Paris-Meudon, 92195 Meudon Cedex, France
e-mail: nicole.vilmer@obspm.fr
[4] Department of Physics, University of Thessaloniki, 54124 Thessaloniki, Greece
e-mail: vlahos@astro.auth.gr

Received 19 November 2003 / Accepted 26 March 2004

Abstract. We present a model for the acceleration and radiation of solar energetic particles (electrons) in evolving complex active regions. The spatio – temporal evolution of active regions is calculated using a cellular automaton model, based on self-organized criticality. The acceleration of electrons is due to the presence of randomly placed, localized electric fields produced by the energy release process, simulated by the cellular automaton model. We calculate the resulting kinetic energy distributions of the particles and their emitted X-ray radiation spectra using the thick target approximation, and we perform a parametric study with respect to number of electric fields present and thermal temperature of the injected distribution. Finally, comparing our results with the existing observations, we find that they are in a good agreement with the observed X-ray spectra in the energy range 100–1000 keV.

Key words. Sun: flares – Sun: X-rays, gamma rays – acceleration of particles

1. Introduction

It is now commonly accepted that solar active regions – domains of strong magnetic fields on the solar surface – are complex dynamical systems. Their evolution is closely related to many solar phenomena, such as coronal heating and solar flares. Solar flares are the manifestations of a sudden and intense energy release process. During solar flares, magnetic energy in the range 10^{28} to 10^{34} erg is released in the solar chromosphere and corona over a few minutes by means of magnetic reconnection. It is clear that understanding the role of the magnetic reconnection process in solar flares is crucial; however, this task is complex and difficult mainly due to the complex magnetic environment associated with this process (for details on magnetic reconnection processes see Priest & Forbes 2000). It is believed that the energy release process during solar flares gives rise to plasma heating, bulk mass motions, and particle (electrons and ions) acceleration.

During the last two decades, due to the existence of several space-born solar instruments and of a number of ground-based solar telescopes, a number of statistical studies of the solar flaring activity has been performed (see e.g., Vilmer 1993; Vilmer & Mackinnon 2003, for reviews). These observations (Dennis 1985; Benz 1985; Benz & Aschwanden 1992; Crosby et al. 1993; Aschwanden et al. 1995; Crosby et al. 1998; Krucker & Benz 1998; Aschwanden et al. 2000) established that the frequency distributions of impulsive events (in particular solar flares) as a function of total energy, peak luminosity and duration are well defined power laws, extending over several orders of magnitude. Several qualitative models have been developed to model the dynamic evolution of solar flares (for reviews see van den Oord 1994; Vlahos 1996; Bastian & Vlahos 1997) following the above observational evidence. These models revealed the necessity of studying and understanding the global behavior of the evolution of the complex active regions and particle acceleration in such a complex environment.

The theoretical work of studying the evolution and the dynamics of complex active regions followed, in general, two different approaches:

(1). MHD numerical simulations (e.g. Galsgaard & Nordlund 1996; Einaudi et al. 1996; Dmitruk et al. 1998; Georgoulis et al. 1998; Galtier & Pouquet 1998; Walsh & Galtier 2000). According to these models, random shearing motions of the magnetic field lines at the photospheric boundary lead to the formation of current sheets inside the

Send offprint requests to: A. Anastasiadis,
e-mail: anastasi@space.noa.gr

active region, where magnetic reconnection occurs. The MHD approach gives a better insight into the small-scale processes (i.e. magnetic reconnection) in active regions, but has difficulty modelling the essential kinetic aspects, as well as the complexity of entire active regions and solar flares. As these simulations are time consuming and can only treat a small number of reconnection events and relatively small volumes, they fail to account for the observed statistical properties of solar flares.

(2). Cellular Automata (CA) models either based on self-organized criticality, (e.g. Lu & Hamilton 1991; Lu et al. 1993; Vlahos et al. 1995; Georgoulis & Vlahos 1996, 1998) or on percolation theory (i.e. probabilistic CA models) (e.g. MacKinnon et al. 1996; MacKinnon & Macpherson 1999; Vlahos et al. 2002). In these models the continuous loading of the active regions with new magnetic flux can produce several magnetic discontinuities. Simple rules were applied for the redistribution of magnetic fields and the release of magnetic energy at these discontinuities. The CA models can rapidly and efficiently treat the complexity of spatially extended systems but they face problems describing in detail the small scale processes that occur (for a recent comprehensive review on CA models see Charbonneau et al. 2001).

Recently, several efforts have been made to connect the two complementary approaches (the MHD simulations and the CA models). Isliker et al. (1998, 2000) revealed the role of several components of CA models, such as the physical interpretations of the grid-variable, the nature of the energy release process, and the role of diffusivity. These efforts lead to a construction of a new type of CA models for solar flares (Isliker et al. 2001) which are compatible with MHD theory and produce statistical results in agreement with the observations. In addition to the above efforts, hybrid models, which are intermediate between CA models and full MHD and reduced MHD models, have been constructed mainly to account for the coronal heating problem (e.g. Einaudi & Velli 1999; Buchlin et al. 2003).

The commonest approach for the particle acceleration models proposed for solar flares (for review on acceleration models see Miller et al. 1997; Anastasiadis 2002) is to decouple the different processes (i.e. energy release, acceleration, transport and radiation). It is clear that in any effort to develop global models for solar flares one must consider the coupling between these different processes. This is not an easy task as these processes have different temporal and spatial scales and usually act simultaneously (see Cargill 2002 for discussion of coupling models). Anastasiadis & Vlahos (1991, 1994) proposed a model for the acceleration of particles (electrons and ions) by an ensemble of shock waves, assuming that the energy is released by means of many localized, small-scale explosive phenomena which were the drivers of a number of shock fronts (small-scale, short-lived discontinuities). In these early models there was still a vague and only qualitative association between the acceleration mechanism and the energy release process.

Anastasiadis et al. (1997) were the first to try to connect the energy release process with the acceleration of electrons in solar flares, using a CA model for the energy release. The acceleration was based on a random number of localized electric fields (super-Dreicer electric fields) closely associated with the energy release process. In the present work our goal is to improve and extend the above model, calculating the electric fields in a more consistent way, using the Ampère law, incorporating the radiation process and comparing our results with the observations. In the next section we outline the basic rules of the CA model, used for the calculation of the energy release time series. In Sect. 3, the acceleration and radiation model is presented, followed by our results for the energy distribution of electrons as well as the corresponding X-ray radiation flux. Finally in Sect. 5 we summarize our results, comparing them with the existing observations, and discuss the possible extensions of our work.

2. The CA model for energy release

For the study of the energy release process we use a 3-D cellular automaton (CA) model based on self-organized criticality. The basic idea is that the evolution of active regions can be simulated by the continuous addition or change of new magnetic flux to the pre-existing magnetic topology, until the local magnetic gradient reaches a threshold. At this point, the local unstable magnetic topology is relaxed by redistributing the excess magnetic field to its nearest neighbors. This redistribution of the magnetic field can cause the lack of stability in the neighbors and the appearance of flares in the form of avalanches on all scales of our system. In the following we only outline the basic rules of the CA model; for a detailed description see Vlahos et al. (1995) and Georgoulis & Vlahos (1998).

The basic rules of the CA model are:
(1) Initial loading;
(2) Ongoing random loading with increment δB given by the probability function:

$$P(\delta B) \approx (\delta B)^{-5/3}; \tag{1}$$

(3) Relaxation due to reconnection of magnetic field, leading to the generation of reconnecting current sheets, according to the equation:

$$\nabla \times \boldsymbol{B} \approx \boldsymbol{J}; \tag{2}$$

(4) Energy release, which is calculated using:

$$\epsilon \approx \left(B_i - \frac{6}{7}B_{\rm cr}\right)^2 \tag{3}$$

where B_i is the value of the magnetic field at a given grid point i, which becomes unstable when $B_i \geq B_{\rm cr}$, where $B_{\rm cr}$ is the critical value of the magnetic field.

Note that the physical interpretation of the above simple rules can be found in Isliker et al. (1998). The selected probability distribution (Eq. (1)) of the driver is a Kolmogorov type spectrum, and $B_{\rm cr} = 10$. Detailed studies of the properties of the CA model when the external driver is variable, as well as for different values of $B_{\rm cr}$ have shown that the values chosen in this study can provide a significant number of flares (avalanches) in

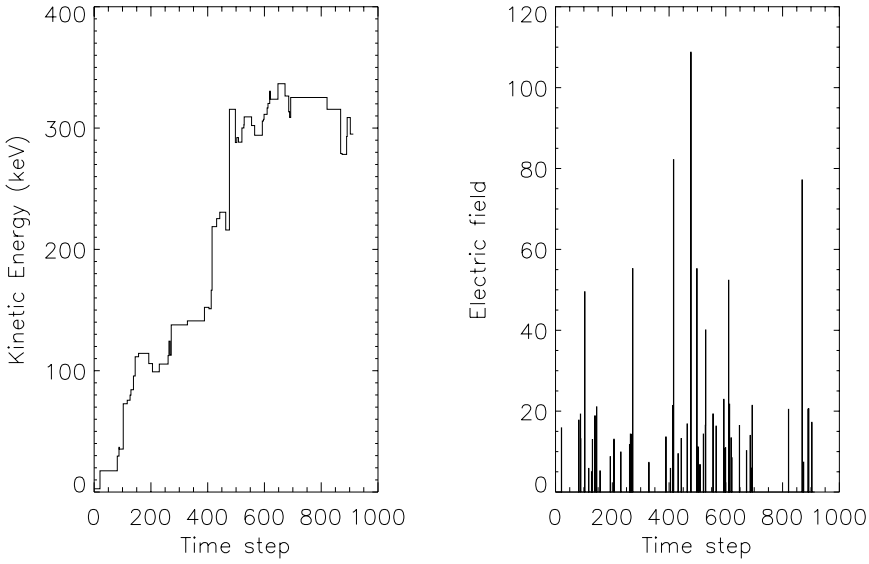

Fig. 1. The temporal evolution of the kinetic energy of a single electron (*on the left*) and the corresponding electric field time series experienced by this electron (*on the right*), for $N = 1000$. Note that the changes in the energy correspond to the variations of the electric field strength, which is normalized to the Dreicer value.

a grid of ($100 \times 100 \times 100$) size (see Georgoulis & Vlahos 1998).

The most important result from the CA model, for our purpose, is that an energy release time series ($\epsilon(t)$) can be constructed using Eq. (3). This time series is highly intermittent, obeys a double power-law frequency distribution, and also exhibits scale-invariant behavior, enclosing a self-similar nature (see Georgoulis & Vlahos 1996; and Fig. 1 of Anastasiadis et al. 1997).

3. Description of the acceleration and radiation model

The most direct and simple way to accelerate particles is by a large scale quasi-static electric field. A number of acceleration models with sub-Dreicer electric fields have been proposed for solar flares (see e.g., Tsuneta 1985; Holman & Benka 1992). These models can explain the bulk energization of electrons up to 100 keV, but they face several problems such as: the requirement of a very extended electric field parallel to the magnetic field or the existence of highly filamented current channels, causing current closure and particle escaping problems. Application of super-Dreicer electric field models to solar flares have also been carried out in the past (e.g., Martens 1988; Litvinenko 1996, 2000). These models invoke a reconnecting current sheet with a significant magnetic field, which, together with the assumed inflow plasma velocity, can produce a convective super-Dreicer electric field. In our model we are following the above approach of the super-Dreicer electric field models.

Litvinenko (1996) was able to calculate the convective electric field in a reconnecting current sheet using the Ampère law and assuming that a particle flow towards the sheet is produced by the electric drift. Following the above assumptions the electric field is given by the relation:

$$E = \frac{B^2}{4\,\pi\,e\,n\,\Delta l} \tag{4}$$

where Δl is the maximum length of the current sheet over which the particles are accelerated and n is the ambient plasma density ($n = 10^{10}$ cm^{-3}).

In our model, we assume that the energy release time series, produced by the CA model through Eq. (3), is closely associated with the presence of a number of reconnecting current sheets in our system. This assumption is based on the fact that the energy release is produced by magnetic reconnection processes, simulated in the CA model by its redistribution rules. As the released energy calculated by the CA model is $\epsilon(t) \sim B^2(t)$ (i.e. Eq. (3)), we can construct a virtual electric field time series ($E(t)$) from the energy release time series using Eq. (4) for the electric field.

Each injected electron enters the acceleration volume and interacts successively with elements of the electric field time series randomly selected from the interval [1, N], performing a free flight between each interaction. At each electron interaction with a reconnecting current sheet, the kinetic energy change is given by the relation:

$$\Delta E_k = \pm\,\alpha\;\; e\,E(t)\,\Delta l \tag{5}$$

where the plus (minus) sign corresponds to in (out of) phase interaction, e is the electron charge, $\Delta l = 10^3$ cm and $E(t)$ the selected element of the virtual electric field time series. The parameter α is selected randomly to vary between zero and one at each interaction and plays the role of the acceleration coefficient, controlling the efficiency of the process.

We must note that in our previous model (Anastasiadis et al. 1997), we estimated the electric field in each reconnecting current sheet using the relation:

$$E = |-\frac{\boldsymbol{v}_{\mathrm{A}} \times \boldsymbol{B}}{c}| \approx 2.184\ 10^3\ B^2(t)\ n^{-1/2} \tag{6}$$

assuming that the ambient plasma flow is of the order of the Alfvèn speed, v_{A}, and that the electric field in the current sheet can be considered as a convective field. This approach led to overestimation of the electric field strengths by a factor of 4 for the used model parameters. We believe that using Eq. (4) we compute the electric fields in a more consistent way (see Litvinenko 1996).

The aim of our acceleration model is to calculate the final kinetic energy distribution of the electrons, by performing a parametric study according to the maximum number of interactions (N). In addition to the acceleration process we wish to compute the resulting X-ray radiation flux. To do so we choose to consider as a first approach that energetic electrons produce thick target radiation (for details see Brown 1971; Vilmer et al. 1982). In other words, we assume that the accelerated electrons, after their escape from the acceleration volume, are injected in a dense medium where they radiate all their energy instantaneously with no modification due to transport.

Following this approach, if we consider an electron of initial energy E_0, the number of photons of energy $h\nu$ is given by:

$$\mu(h\nu, E) = \int_{E_0}^{h\nu} \sigma(h\nu, E)\, n_{\mathrm{p}}\, v(E)\, \frac{\mathrm{d}E}{\mathrm{d}t}\, \mathrm{d}t \tag{7}$$

where $\sigma(h\nu, E)$ is the cross-section coefficient of the bremsstrahlung emission, n_{p} is the density of the ambient plasma, $v(E)$ is the velocity of the particle and $\frac{\mathrm{d}E}{\mathrm{d}t}$ is the energy loss due to collisions. Then, the emitted flux of an initial energy distribution of electrons $F(E_0)$ in the range E_0, $E_0 + \mathrm{d}E$ is given by the relation:

$$I(h\nu) = \int_{h\nu}^{+\infty} F(E_0)\, \mu(h\nu, E_0) \mathrm{d}E_0. \tag{8}$$

In the next section, we present our results concerning the final kinetic energy of the electrons and their emitted X-ray radiation spectra as a function of the maximum number of interactions (N) and the thermal temperature of the injected distribution.

4. Results

As was stated earlier in our model description, each electron performs a free flight between electric fields of variable strength, selected randomly from a time series that is highly intermittent. At each encounter, if the randomly selected element of the time series is non-zero, electrons lose or gain energy in a nonsystematic way, according to Eq. (5).

In Fig. 1 the temporal evolution of the kinetic energy of a single electron with initial kinetic energy 3.45 keV is presented (on the left) together with the corresponding part of the electric field time series (on the right) with which this electron interacts. The electric field is normalized to the Dreicer electric field value ($E_{\mathrm{D}} \approx 6 \times 10^{-5}$ V cm^{-1}). As can be clearly seen, the electric field strengths locally exhibit large variations that lead to dramatic changes of the kinetic energy of electrons. Note that, although the maximum number of interactions is $N = 1000$, the non-zero electric fields are fewer, this means that the number of interacting current sheets is not equal to the maximum number of interactions N. We will address this point at the end of this section.

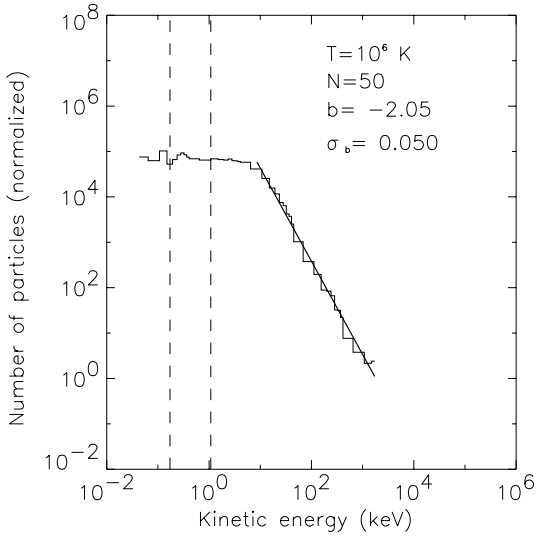

Fig. 2. The average kinetic energy distribution of accelerated electrons for the case of $N = 50$ and $T_1 = 10^6$ K. The fit is given by Eq. (9) and the vertical dashed lines indicate the injected kinetic energy range.

We are interested in following the evolution of a Maxwellian type velocity distribution of electrons (i.e. $f(v)$), by injecting electrons into our acceleration volume, with initial velocity in the range $2 \leq (v/V_{\mathrm{e}}) \leq 5$, where V_{e} is the thermal velocity. We consider two different temperatures: $T_1 = 10^6$ K corresponding to $V_{\mathrm{e1}} = 3.88 \times 10^8$ cm s^{-1} and $T_2 = 10^7$ K corresponding to $V_{\mathrm{e2}} = 1.23 \times 10^9$ cm s^{-1}. The resulting thermal kinetic energies are 43 eV and 430 eV, respectively.

We want to calculate the resulting kinetic energy distributions by performing a parametric study with respect to the maximum number N for the two different initial injected Maxwellian distributions. We normalize the injected distributions in such a way that $f(5V_{\mathrm{e}}) = 1$ and follow numerically the kinetic energy change of 1000 electrons in every injected velocity bin. To eliminate any effect from the random numbers used in our numerical code, all the presented energy distributions are averaged over 10 sample runs with the same parameters. In Figs. 2 and 3 we present the numerically evaluated kinetic energy distribution (average of 10 sample runs) for $N = 50$ for $T_1 = 10^6$ K and for $T_1 = 10^7$ K respectively. Similarly in Figs. 4 and 5 the energy distributions for $N = 1000$ are presented. Note that the vertical dashed lines in these figures indicate the initially injected kinetic energy range.

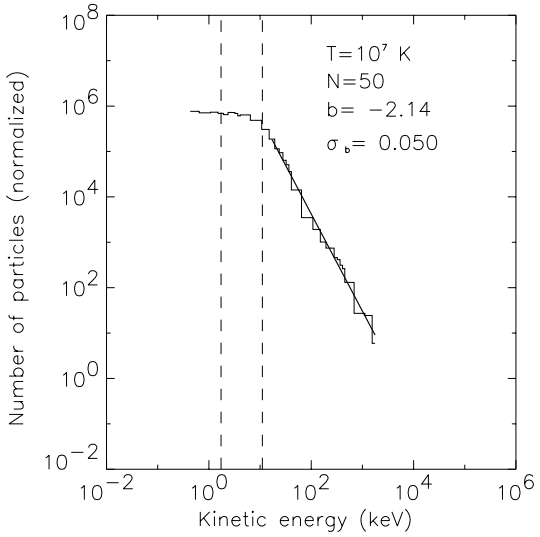

Fig. 3. Same as Fig. 2, but for $T_2 = 10^7$ K.

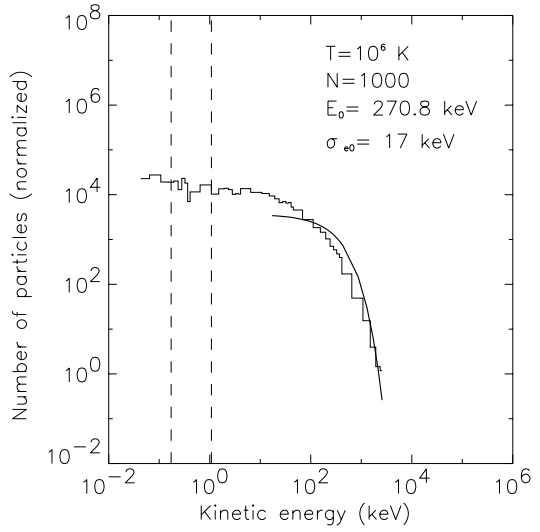

Fig. 4. The average kinetic energy distribution of accelerated electrons for the case of $N = 1000$ and $T_1 = 10^6$ K. The fit is given by Eq. (10).

All of our resulting average kinetic energy distributions can be fitted for kinetic energies above 10 keV, either with a power law function of the form:

$$F(E_\mathrm{k}) \approx E_\mathrm{k}^{-b} \tag{9}$$

or with an exponential function of the form:

$$F(E_\mathrm{k}) \approx \exp\left(-\frac{E_\mathrm{k}}{E_\mathrm{o}}\right) \tag{10}$$

where the calculated values of the index of the power law b and the characteristic kinetic energy E_o, together with their standard deviations are given in Table 1. The maximum kinetic energy reached by the electrons is of the order of few MeV. This value is connected with the strength of the selected electric fields and does not increase considerably with the increase

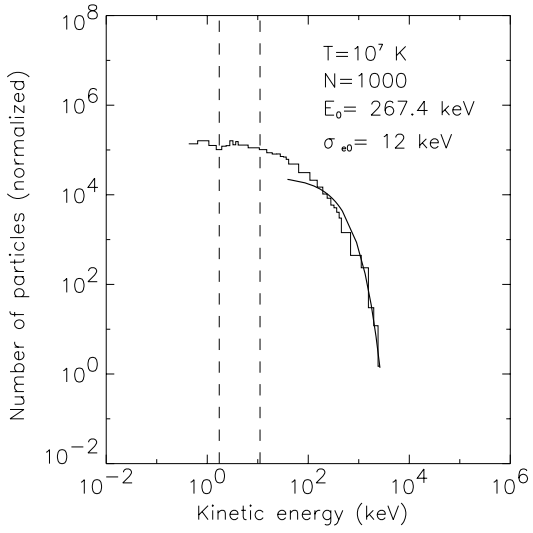

Fig. 5. Same as Fig. 4, but for $T_2 = 10^7$ K.

Table 1. Summary of the estimated values of the power law index b of Eq. (9) and of the characteristic energy E_o of Eq. (10) together with their corresponding dispersions σ_b and σ_Eo for different maximum N and the two temperatures used.

T [K]	N	b	σ_b	E_o [keV]	σ_Eo [keV]
	50	2.05	0.005		
	200	1.96	0.064		
10^6	500	1.96	0.142		
	700			218.5	11.0
	1000			270.8	17.0
	50	2.14	0.050		
	200	2.05	0.073		
10^7	500	1.79	0.095		
	700	2.35	0.224		
	1000			267.4	12.0

of the maximum number of interactions N. On the other hand, as is shown in Fig. 6, when N increases, for a given temperature the relative number of electrons above 100 keV also increases. In addition, for a given N the relative number of electrons above 100 keV increases with the temperature of the injected distribution. Finally, our results indicate that as the maximum number of interactions (N) increases the resulting energy distributions diverge from well defined power laws and an exponential tail develops.

In Fig. 7 we present the X-ray spectra estimated using Eq. (8), for the electron energy distributions given in Figs. 2 (lower curve in the figure) and 5 (higher curve in the figure). The fitting was done by a power law in the energy ranges 10–100 keV (considered as the low energy part) and 100–1000 keV (considered as the high energy part). In Fig. 8 we present in a form of scatter plots our results for the power law index of the calculated X-ray spectra with respect to the maximum number N for the two temperatures used. For the low energy range (10–100 keV) the mean value of the index

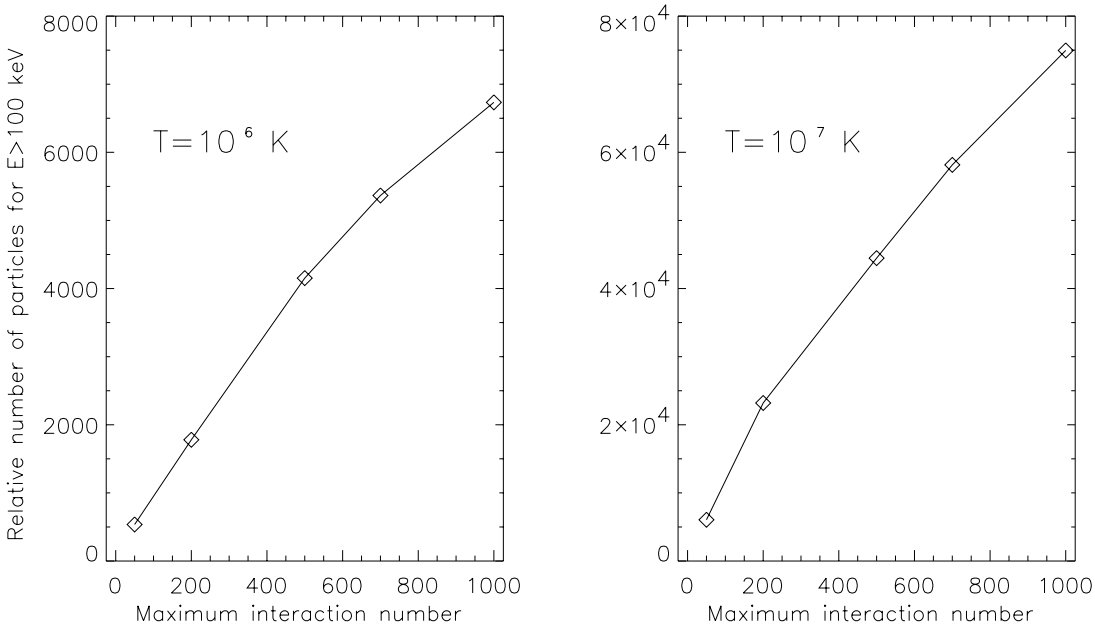

Fig. 6. The estimated relative number of electrons with kinetic energies above 100 keV, as a function of maximum number of interactions, for the temperatures used.

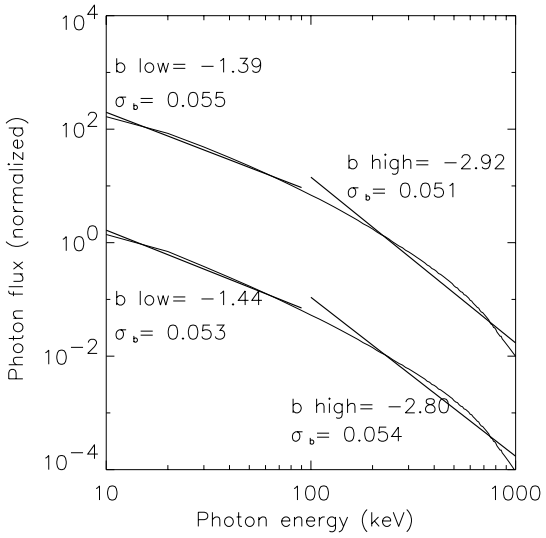

Fig. 7. The calculated X-ray radiation spectra of the resulting electron distributions given in Figs. 2 (lower curve in the figure) and 5 (higher curve in the figure). The fitting was performed in two energy ranges 10–100 keV and 100–1000 keV and is given by power laws.

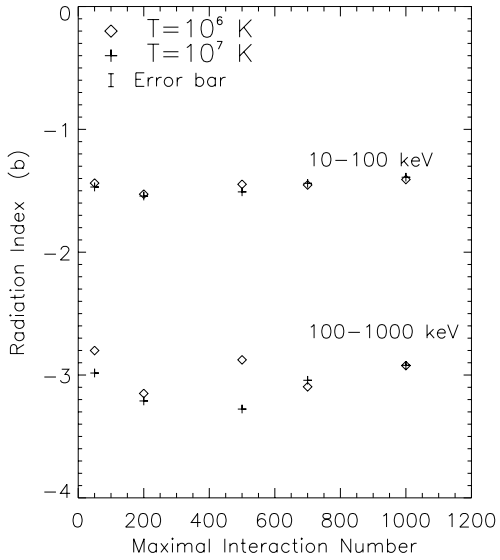

Fig. 8. Scatter plots summarizing our results concerning the power law index of the emitted X-ray radiation as a function of the maximum number N.

is −1.45 for $T_1 = 10^6$ K and −1.47 for $T_2 = 10^7$ K, while for the high energy part (100–1000 keV) the mean values are −2.96 and −3.08 respectively. From Fig. 8 we can conclude that the power law indices of the calculated X-ray spectra are almost independent of the variations of the selected number of maximum interactions (N) and the temperatures used.

Finally we address the question of how many interactions with the reconnecting current sheets the injected electrons perform. This is an important question as the maximum number N used so far is not representative of the number of current sheets, but corresponds to the maximum number of randomly selected elements from the electric field time series. To address this question we calculated the number of non-zero electric fields with which all the particles of the injected distribution interact out of the randomly selected N elements. In Fig. 9 we present the calculated probability of the number of interactions (i.e. number of reconnecting current sheets) that the initial injected electron distribution experiences

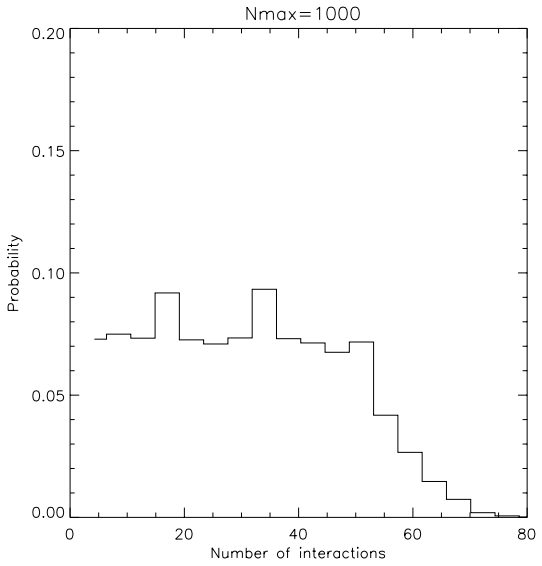

Fig. 9. The probability distribution function of the number of reconnecting current sheets that the injected electron distribution experiences if $N = 1000$.

for $N = 1000$. This probability is a continuous function, as it is related to the uniform random number generator function used to select the N elements of the time series. An interesting point that we must investigate in the future is to consider different types of probability functions for the number of current sheets.

5. Summary and discussion

In this work we considered a global model for the acceleration and radiation process of electrons in complex evolving active regions. Considering that the evolution of active regions can be simulated by the evolution of a Cellular Automaton (CA) model based on self-organized criticality, we tried to connect the energy release process occurring in solar flares with the acceleration and radiation processes of energetic electrons.

We assumed that the acceleration of electrons is based on the presence of a number of reconnecting current sheets, which are produced by the energy release process inside the active regions. These current sheets are randomly placed super-Dreicer electric fields of variable strengths, connected with the energy release time series produced by our CA model. We have performed a parametric study with respect to the maximum number of interactions (N) and the initial temperature of the injected electron distribution. Electrons can be accelerated up to a few MeV and their resulting energy distributions can be fitted either with a power law, or with an exponential distribution. Our investigation showed that as N increases, it affects the shape of the energy distribution, which begins to diverge from a well defined power law, and an exponential tail develops. The above result is consistent with the one found in our early work (Anastasiadis et al. 1997). Furthermore, we found that for a given temperature the total number of accelerated electrons above 100 keV also increases as N increases.

In addition to the acceleration, in this work we studied the radiation process by calculating the emitted X-ray spectra of the resulting electron distributions. We used the thick target approximation, assuming that electrons after their acceleration are injected in a dense medium where they radiate away all their energy. The calculated spectra were fitted with a power law in a low energy range (10–100 keV) and in a high energy range (100–1000 keV) (see Fig. 7). Our results (see Fig. 8) indicate that the power law indices of the X-ray spectra, remain almost constant with respect to the variations of the maximum number of interactions (N) and the temperatures used.

As a general remark, the X-ray spectrum in the low energy part of the spectrum is much flatter than really observed (spectral index greater than −2). Statistical studies of Crosby et al. (1993) and Bromund et al. (1995) have indeed shown that photon spectra observed with scintillators are between −2 and −7 above 30 keV, the mean value between 25 and 200 keV being −3.9 (Vestrand 1988). This is probably due to the neglect of Coulomb collisions in the model, which should decrease the number of low energy electrons. On the other hand the values obtained in the photon energy range 100–1000 keV (see Fig. 8) appear reasonable when compared to observations (i.e. they indeed lie around −3). Photon spectra observed with SMM between 300 keV and 1 MeV have power law spectra between −2 and −5 with a mean value of −2.9 (Vestrand 1988) which could be consistent with some of the spectra shown in this paper. With Phebus on GRANAT, photon power law spectra in the (−2.8, −3) range have also been observed from 300 to 500 keV. However, the spectrum was found to become flatter above a few MeV, which is not predicted here. Finally, RHESSI observed photon spectra around −2.2–−2.3 – between 10 and 100 keV (still steeper than what is predicted here) with a steepening towards −3 above 30 keV (Krucker & Lin 2002).

As a conclusion, the predicted spectrum seems to be consistent with some observations (at least for the higher part of the predicted spectrum where Coulomb energy losses play a less significant role). The hardness of the predicted spectrum above 100 keV may be consistent with what is observed but the magnitude of the photon flux should also be produced.

More work is clearly needed in the future if we want to incorporate the transport of the particles and to include the radiation losses due to collisions inside the acceleration volume (i.e. use of the thin target emission). This approach can be done if we consider the newly developed CA model -named extended CA- (X-CA) (Isliker et al. 2001), taking advantage of the consistent calculation of the magnetic and electric fields in the simulation box. In this direction, studies for the case of a random walk process in a environment which has fractal properties, like the one produced by the CA models, are currently under way (see Isliker & Vlahos 2003). We believe that much effort should be put into developing global models for the study of the solar corona that can couple the different processes, occurring on different temporal and spatial scales. This approach will open a new highly promising and challenging field for solar physics research.

Acknowledgements. We would like to thank Dr. H. Isliker and Dr. M. Georgoulis for many stimulating discussions on cellular automata models and their applications to solar flares. C.G. would also

like to thank the Research Committee of the Academy of Athens for their support. This work was partially supported by the Greek General Secretariat for Research and Technology.

References

Anastasiadis, A. 2002, J. Atm. Solar – Terr. Phys., 64(5-6), 481
Anastasiadis, A., & Vlahos, L. 1991, A&A, 245, 271
Anastasiadis, A., & Vlahos, L. 1994, ApJ, 428, 819
Anastasiadis, A., Vlahos, L., & Georgoulis, M. K. 1997, ApJ, 489, 367
Aschwanden, M. J., Tarbell, T. D., Nightingle, R. W., et al. 2000, ApJ, 535, 1047
Aschwanden, M. J., Montello, M., Dennis, B. R., & Benz, A. O. 1995, ApJ, 440, 394
Bastian, T. S., & Vlahos, L. 1997, in Lecture Notes in Physics, ed. G. Trottet (Springer-Verlag), 483, 68
Benz, A. O. 1985, Sol. Phys., 96, 357
Benz, A. O., & Aschwanden, M. J. 1992, in Lecture Notes in Physics, ed. Z. Svestka et al. (Springer-Verlag), 399, 106
Bromund, K. R., McTiernan, J. M., & Kane, S. R. 1995, ApJ, 455, 733
Brown, J. C. 1971, Sol. Phys., 18, 489
Buchlin, E., Aletti, V., Galtier, S., Velli, M., et al. 2003, A&A, 406, 1061
Cargill, P. J. 2002, in SOLMAG: Magnetic Coupling of the Solar Atmosphere, ESA SP-505, 245
Charbonneau, P., McIntosh, S. W., Lui, H.-L., & Bogdan, T. 2001, Sol. Phys., 203, 321
Crosby, N. B., Aschwanden, M. J., & Dennis, R. B. 1993, Sol. Phys., 143, 275
Crosby, N. B., Vilmer, N., Lund, N., & Sunyaev, R. 1998, A&A, 334, 299
Dennis, B. R. 1985, Sol. Phys., 100, 465
Dmitruk, P., Gomez, D. O., & DeLuca, E. E. 1998, ApJ, 505, 974
Einaudi, G., & Velli, M. 1999, Phys. Plasmas, 6, 4146
Einaudi, G., Velli, M., Politano, H., & Pouquet, A. 1996, ApJ, 457, L13
Galsgaard, K., & Nordlund, A. 1996, J. Geophys. Res., 101, 13445
Galtier, S., & Pouquet, A. 1998, Sol. Phys., 179, 141
Georgoulis, M., & Vlahos, L. 1996, ApJ, 469, L135
Georgoulis, M., & Vlahos, L. 1998, A&A, 336, 721
Georgoulis, M., Velli, M., & Einaudi, G. 1998, ApJ, 497, 957
Holman, G. D., & Benka, S. G. 1992, ApJ, 400, L79
Isliker, H., Anastasiadis, A., Vassiliadis, D., & Vlahos, L. 1998, A&A, 335, 1085
Isliker, H., Anastasiadis, A., & Vlahos, L. 2000, A&A, 361, 1134
Isliker, H., Anastasiadis, A., & Vlahos, L. 2001, A&A, 377, 1068
Isliker, H., & Vlahos, L. 2003, Phys. Rev. E, 67, 026413
Krucker, S., & Benz, A. O. 1998, ApJ, 501, L213
Krucker, S., & Lin, R. P. 2002, Sol. Phys., 210, 229
Lu, E. T., & Hamilton, R. J. 1991, ApJ, 380, L89
Lu, E. T., Hamilton, R. J., McTierman, J. M., & Bromund, K. R. 1993, ApJ, 412, 841
Litvinenko, Y. E. 1996, ApJ, 462, 997
Litvinenko, Y. E. 2000, Sol. Phys., 194, 324
MacKinnon, A. L., Macpherson, K. P., & Vlahos, L. 1996, A&A, 310, L9
Macpherson, K. P., & MacKinnon, A. L. 1999, A&A, 350, 1040
Martens, P. C. 1988, ApJ, 330, L131
Miller, J. A., Cargill, P. J., Emslie, A., et al. 1997, J. Geophys. Res., 102, 14631
Priest, E. R., & Forbes, T. 2000, Magnetic Reconnection, MHD Theory and Applications (Cambridge Univercity Press)
Tsuneta, G. D. 1985, ApJ, 290, L353
van den Oord, G. H. J. 1994, Fragmented Energy Release in Sun and Stars (Kluwer)
Vestrand, W. T. 1988, Sol. Phys., 118, 95
Vilmer, N., & MacKinnon, A. L. 2003, in Energy Conversion and Particle Acceleration, ed. K.-L. Klein (Springer-Verlag), 127
Vilmer, N. 1993, Adv. Space Res., 13(9), 221
Vilmer, N., Kane, S. R, & Trottet, G. 1982, A&A, 108, 306
Vilmer, N., & Trottet, G. 1997, in Lecture Notes in Physics, ed. G. Trottet (Springer-Verlag), 483, 28
Vlahos, L. 1996, in Radio Emission from the Stars and the Sun, ed. A. R. Taylor, & J. M. Paredes (ASP Press), ASP Conf. Ser., 93, 355
Vlahos, L., Fragos, T., Isliker, H., & Georgoulis, M. 2002, ApJ, 575, L87
Vlahos, L., Georgoulis, M. K., Kluiving, R., & Paschos, P. 1995, A&A, 299, 897
Walsh, R. W., & Galtier, S. 2000, Sol. Phys., 197, 57